

Intensive terahertz emission from GaSe_{0.91}S_{0.09} under collinear difference frequency generation

Jingguo Huang, Zhiming Huang, Jingchao Tong, Cheng Ouyang, Junhao Chu et al.

Citation: *Appl. Phys. Lett.* **103**, 081104 (2013); doi: 10.1063/1.4818764

View online: <http://dx.doi.org/10.1063/1.4818764>

View Table of Contents: <http://apl.aip.org/resource/1/APPLAB/v103/i8>

Published by the AIP Publishing LLC.

Additional information on *Appl. Phys. Lett.*

Journal Homepage: <http://apl.aip.org/>

Journal Information: http://apl.aip.org/about/about_the_journal

Top downloads: http://apl.aip.org/features/most_downloaded

Information for Authors: <http://apl.aip.org/authors>

ADVERTISEMENT



**MATERIAL SCIENCE RESEARCH
AT 3K – MADE SIMPLE**

MONTANA INSTRUMENTS
COLD SCIENCE MADE SIMPLE

CLOSED CYCLE OPTICAL CRYOSTATS

Intensive terahertz emission from GaSe_{0.91}S_{0.09} under collinear difference frequency generation

Jingguo Huang,¹ Zhiming Huang,^{1,2,a)} Jingchao Tong,¹ Cheng Ouyang,¹ Junhao Chu,¹ Yury Andreev,^{3,4} Konstantin Kokh,⁵ Grigory Lanskii,^{3,4} and Anna Shaiduko^{3,4}

¹National Laboratory for Infrared Physics, Shanghai Institute of Technical Physics, CAS, Shanghai 200083, China

²Key Laboratory of Space Active Opto-Electronics Technology, Shanghai Institute of Technical Physics, CAS, Shanghai 200083, China

³Institute of Monitoring of Climate and Ecological Systems, SB RAS, Tomsk 634055, Russia

⁴Laboratory of Advanced Materials and Technologies, Siberian Physical-Technical Institute of Tomsk State University, 1 Novosobornaya Sq., Tomsk 634050, Russia

⁵Laboratory of Crystal Growth, Institute of Geology and Mineralogy, SB RAS, Novosibirsk 630090, Russia

(Received 14 May 2013; accepted 2 August 2013; published online 20 August 2013)

An intensive, broad tunable monochromatic Terahertz (THz) emission is generated from S-doped (2 wt. %) GaSe (solid solution GaSe_{0.91}S_{0.09}) crystals by collinear difference frequency generation method. The generated THz signal of 3.8 ns covers the spectral range of 0.57–3.57 THz (84.0–528.0 μm), with a maximal THz output peak power of 21.8 W at 1.62 THz. The THz power conversion efficiency is of 45% higher than that of undoped GaSe, which is mainly contributed to the improved optical properties. The terahertz source is of great potential to be exploited for the out-of-door applications due to the increased crystal hardness. © 2013 AIP Publishing LLC. [<http://dx.doi.org/10.1063/1.4818764>]

Intensive Terahertz (THz) source is always pursued for the potential applications in terahertz communication,¹ high resolution spectral imagination,² and THz radar.³ Difference frequency generation (DFG) is an important way to generate high power, narrow bandwidth, broad range, continuously tunable, and coherent THz emission by using two tunable ns lasers with slightly different output wavelength. DFG offers the advantages⁴ of relative compactness, technical simplicity, and much stable THz output. This approach has been demonstrated in many nonlinear crystals, such as GaSe,⁴ ZnGeP₂,^{5,6} GaP,⁷ and DAST.⁸

Among them, ε-polytype GaSe ranks the most efficient nonlinear material for frequency converters due to the wonderful physical properties, such as high nonlinear coefficient ($d_{22} = 54$ pm/V), wide transparent spectral range (0.65 to 18 μm and ≥ 50 μm), large birefringence and minimal optical losses in the THz wave range. Nearly the entire frequency range of the output beam (mid-IR (MIR), THz, and millimeter waves) has been achieved by GaSe.⁹ However, GaSe is a very soft and easy cleaving crystal due to the layered structure. The crystal hardness is almost zero in the Mohs scale, which makes it difficult to be cut and polished at arbitrary direction. This is a major factor that hinders this THz source for practical applications.

Fortunately, GaSe is an excellent matrix material for doping with isovalent elements, such as S, In, Te, Al, Er,^{10–14} or pair of different group chemical elements.¹⁵ Its mechanical and optical properties could be significantly improved by doping. Doped crystals showed a large increase (≥ 1.5 times) in the crystal hardness to that of pure GaSe.¹⁵ Among the doped crystals, reasonable concentration of S-doped GaSe crystal presents the promising property for the

THz applications due to the modified physical properties. It includes decreased optical losses due to the less point defects and layer stacking faults, increased thermal conductivity, damage threshold and crystal hardness. Optimal S-doping within 2 to 3 wt. % range is estimated from the maximal frequency conversion efficiency in mid-IR.¹⁰ Although 2 wt. % S-doped GaSe crystal or solid solution crystal GaSe_{0.91}S_{0.09} was well investigated for the optical property in the THz wave range by the THz time domain spectrometer (THz-TDS), and even for THz emission with optical rectification method.¹⁶ However, to the best of our knowledge, the THz wave generation by DFG method has not been reported yet in any doped GaSe crystal. In this letter, we choose a large GaSe_{0.91}S_{0.09} crystal for the THz generation experiment by DFG. This kind of THz source can break down the barriers for the out-of-door applications.

Fig. 1 illustrates the schematic experimental setup of the THz wave generation in GaSe_{0.91}S_{0.09} crystals by collinear difference frequency generation. The fundamental pump is a 1064-nm beam of a Q-switched Nd:YAG laser with the pulse duration ~ 7.8 ns, repetition rate 10 Hz, and spectral bandwidth ~ 0.003 cm⁻¹. The secondary pump for the DFG, is an orthogonal polarized signal beam emitted from an optical parametric oscillator (OPO) pumped by the frequency-tripled ($\lambda = 355$ nm) emission of the same Nd:YAG laser: tunability from 1060 to 1080 nm, line bandwidth ~ 0.075 cm⁻¹, and pulse duration ~ 3.8 ns. The spot shape-form for the two pump beams is semi-circle, with the beam radii of 1.60 and 1.81 mm, respectively. And they are combined in the 2.6×3.7 mm² spot on the crystal surface with a small overlapped beam area of ~ 2.9 mm² through a polarized beam splitter. Additional optical delay line for the 1064-nm beam is used to compensate for the optical pass of the signal beam inside the OPO system to make sure that they arrive at the GaSe_{0.91}S_{0.09} crystal simultaneously. In this experiment,

^{a)}Corresponding author: Zhiming Huang. Electronic mail: zmhuang@mail.sitp.ac.cn

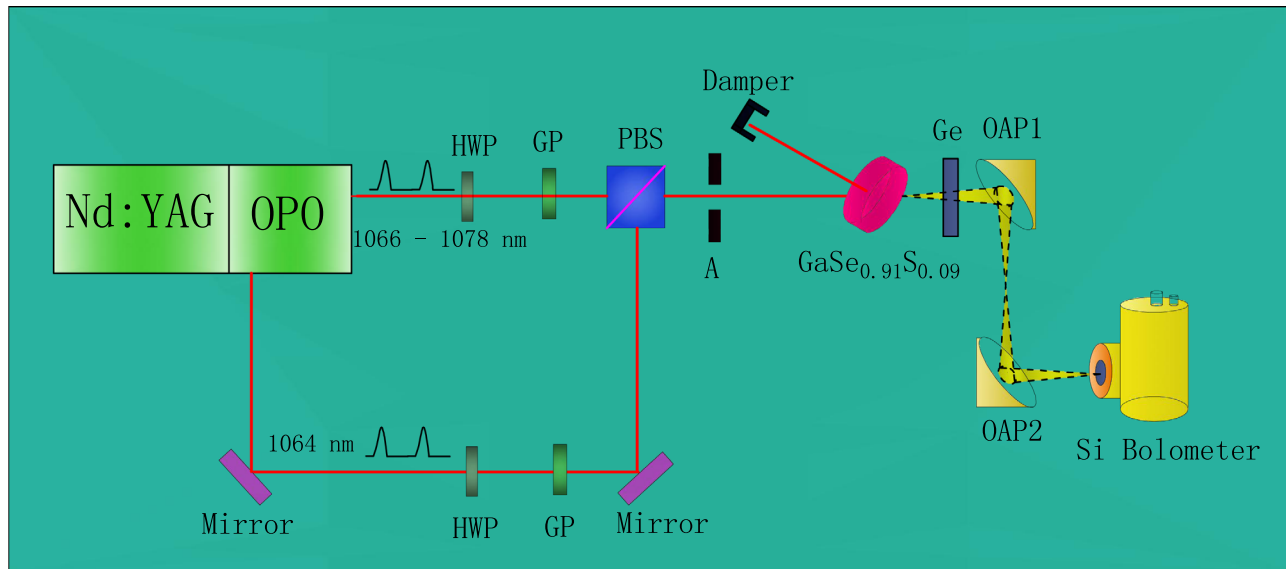


FIG. 1. A schematic experimental setup of the THz wave generation in $\text{GaSe}_{0.91}\text{S}_{0.09}$; OPO is the optical parametric oscillator; HWP is a half wave plate; GP is a Glan prism; PBS is a polarizing beam splitter; A is an aperture; OAP is an off-axis parabolic mirror.

we use the same pulse energy (5 mJ) for the fundamental and OPO signal pump beams. The peak intensity for the fundamental pulse is of $\sim 11.6 \text{ MW/cm}^2$, and that for the signal wave pulse is of $\sim 22.6 \text{ MW/cm}^2$. The total peak intensity is well below the crystal damage threshold. A large as-cleaved off $\text{GaSe}_{0.91}\text{S}_{0.09}$ crystal from the grown boule (z-cut) is used for this THz DFG experiment without additional treatment. It is of 5.5 mm in length and a rectangular input facet with the long and short sides to be of about 30 and 20 mm, respectively. The crystal is mounted on a two-dimensional high-precision rotation stage. The generated THz wave is separated from the pump beams by two 1.5-mm Ge filters, collected by a pair of off-axis parabolic golden mirrors, and then focused onto a liquid helium-cooled Si bolometer. The electrical signal produced by the bolometer is recorded and averaged 10 times in a high speed oscilloscope (LeCroy Wave Runner 62Xi-A). The energy for the generated THz pulse is measured by the value of the electric signal.

In the experiment, a monochromatic THz wave is observed in the oe-e phase matching (PM) configuration, whereas the 1064 nm, OPO signal, and THz wave beams are corresponding to the ordinary (o), extraordinary (e), and extraordinary (e) waves, respectively. Since the terahertz absorption coefficient of e-wave is much smaller than that of o-light inside GaSe,¹⁷ it is reasonable for us to detect this strong e-polarized THz wave, which is testified by a homemade metal grating. The wavelength and spectral bandwidth of the THz wave were verified by a Fourier transform infrared spectrometer with a step-scan method.¹⁸ In the DFG process, the efficient nonlinear coefficient depending on the azimuthal angle θ and φ can be expressed as

$$d_{\text{eff}}^{\text{oe-e}} = d_{22} \cos^2(\theta) \cos(3\varphi), \quad (1)$$

where $d_{22}(\text{GaSe}_{0.91}\text{S}_{0.09}) = 0.89d_{22}(\text{GaSe})$,¹⁰ $\varphi = 0$ for the maximal value of $d_{\text{eff}}^{\text{oe-e}}$.

Fig. 2 gives the external PM angle versus the output THz wavelength. The maximal peak power of the emitted THz wave is achieved both by varying the crystal azimuthal

angle and tuning the signal wavelength simultaneously. When the PM angle is changed from 7.2° to 21.4° and the OPO signal wavelength is in the range from 1066.3 to 1077.8 nm, the central wavelength of the terahertz emission is tuned from 528.0 to $84.0 \mu\text{m}$ (0.57–3.57 THz). To calculate the PM curve theoretically, the exact value of the refractive index in both IR and THz ranges must be known. It is well-known that the refractive index of the S-doped crystal could be estimated by using adequate dispersion relations for the refractive indices of GaSe and GaS from the following equation:¹⁹

$$n^2(\text{GaS}_x\text{Se}_{1-x}) = (1-x)n^2(\text{GaSe}) + xn^2(\text{GaS}). \quad (2)$$

Based on the Sellmeier equation of GaS¹⁹ and GaSe,²⁰ we calculated the theoretical PM angle curve of oe-e type in $\text{GaSe}_{0.91}\text{S}_{0.09}$ (Fig. 2). In the figure, the measured PM curve is agreed with the theoretical calculation. The small difference between them is probably due to two reasons: (a) the

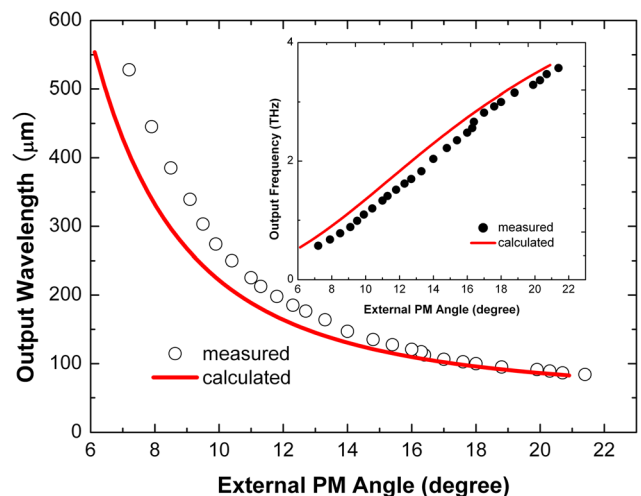


FIG. 2. Output THz wavelength versus the external oe-e type PM angle in $\text{GaSe}_{0.91}\text{S}_{0.09}$ (measured: open circle; calculated: red solid line). Inset: THz frequency versus the external PM angle (measured: solid circle; calculated: red solid line).

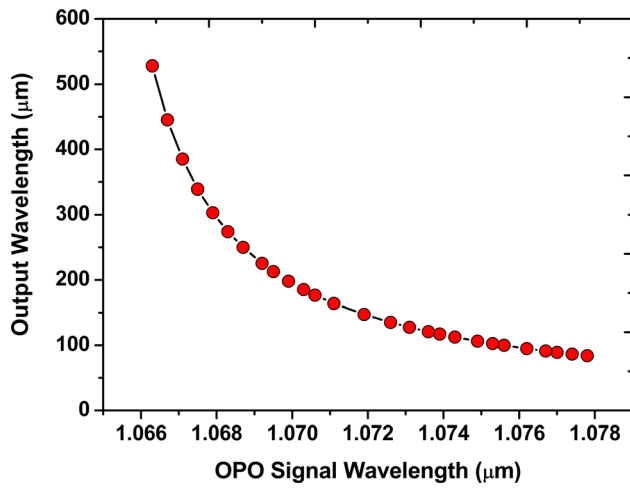


FIG. 3. Output terahertz wavelength versus OPO signal wavelength.

difference between the bulk and surface composition measured by X-ray microanalysis; (b) the real refractive index in the GaSe_{0.91}S_{0.09} crystal used in the THz wave range is substituted by the refractive index of GaSe since the refractive equation of GaS crystal in the MIR range¹⁹ could not be applied in the THz range.

Fig. 3 gives the dependence of the THz wavelength on the OPO signal wavelength. This THz radiation has a pulse duration of ~ 3.8 ns with a repetition rate of 10 Hz. The measured THz output peak power versus the wavelength is shown in Fig. 4, which is corrected for optical losses caused by the absorption of air and two Ge filters. The maximal THz peak power achieved is of 21.8 W at 185.2 μ m (1.62 THz), corresponding to the power conversion efficiency of 6.54×10^{-5} and photon conversion efficiency of 1.14%.

The theoretical THz power conversion efficiency can be calculated from the well-known formula²¹

$$\frac{P_3}{P_1} = 2 \left(\frac{\mu_0}{\epsilon_0} \right)^{\frac{1}{2}} \frac{\omega_3^2 d_{\text{eff}}^2 L^2}{n_1 n_2 n_3 c^2} \left(\frac{P_2}{A} \right) T_1 T_2 T_3 \exp(-\alpha_3 L) \times \frac{1 + \exp(-\Delta\alpha L) - 2\exp(-\Delta\alpha L/2)\cos(\Delta k L)}{(\Delta k L)^2 + (\Delta\alpha L/2)^2}, \quad (3)$$

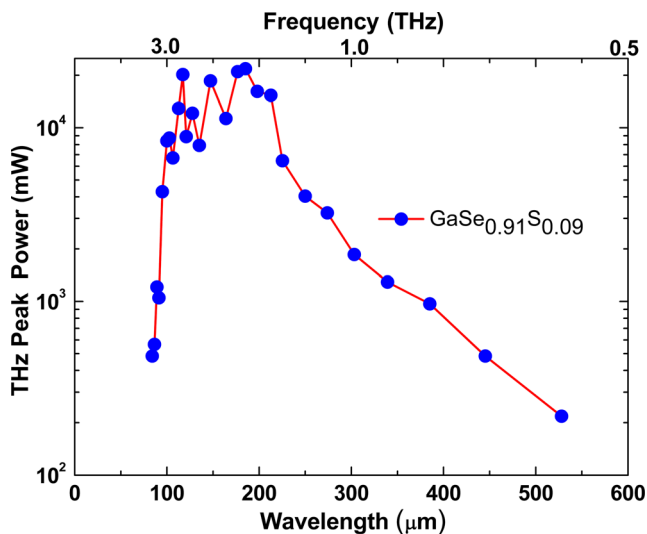


FIG. 4. Output terahertz peak power versus THz wavelength in GaSe_{0.91}S_{0.09}.

where μ_0 and ϵ_0 are the vacuum magnetic permeability and dielectric permittivity, respectively; ω_3 is the output THz frequency; d_{eff} is the effective non-linear optical coefficient; L is the crystal thickness; $\frac{P_2}{A}$ is the input peak intensity of the OPO signal wave; n_i ($i = 1, 2, 3$) is the refractive index at the 1064 nm, OPO signal, and THz wavelengths, respectively; T_i is relative transmission coefficient, given by $T_i = 4n_i/(n_i + 1)^2$; $\Delta\alpha = |\alpha_1 + \alpha_2 - \alpha_3|$ is the differential absorption coefficient depending on the magnitude of the absorption coefficients at the 1064 nm pump, OPO signal, and THz waves. Here, parameters are $\theta_{\text{ext}} = 12.3^\circ$, $d_{\text{eff}} = 53.7$ pm/V, $L = 5.5$ mm, $\frac{P_2}{A} = 22.6$ MW/cm², $n_1 = 2.7$, $n_2 = 2.45$, $n_3 = 3.28$, $\alpha_1 = \alpha_2 \approx 0$, $\alpha_3 \approx 1$ cm⁻¹ at 1.6 THz, $\Delta k = 0$. According to Eq. (3), the theoretical THz power conversion efficiency of GaSe is calculated about 8.0×10^{-5} under the consideration of that only half peak intensity of OPO signal wave is contributed to the THz power generation. As mentioned above, additional 21% decrease occurred in the THz power conversion efficiency for GaSe_{0.91}S_{0.09} due to the 11% decrease of d_{22} . So the theoretical THz power conversion efficiency of GaSe_{0.91}S_{0.09} is estimated about 6.3×10^{-5} , which is well in coincidence with the measured result.

Compared with the highest THz power conversion efficiency generated in GaSe reported by Shi *et al.* with similar crystal length⁴ (1.77×10^{-5} in 4 mm and 4.5×10^{-5} in 7 mm), an over 45% power conversion efficiency is achieved in GaSe_{0.91}S_{0.09} crystal. This is mainly contributed to the improved optical properties at both near-IR (NIR) and THz regions. Fourier transform transmission spectrum in NIR region shows that the reflective index of GaSe_{0.91}S_{0.09} (2.48) is 8% smaller than that of the pure one (2.70) at the pump region. And the reflective index of GaSe_{0.91}S_{0.09} (3.16) at THz region is 4% smaller than that of GaSe (3.28). From Eq. (3), this will introduce a 35% increase in the THz power conversion efficiency in GaSe_{0.91}S_{0.09}, which is larger than that decreased by the effect of small d_{22} . Besides, the absorption coefficient at NIR region could not be ignored for such a thick crystal (5.5 mm). In fact, the absorption coefficient of GaSe_{0.91}S_{0.09} (0.49 cm⁻¹) is much smaller than that of pure one (0.85 cm⁻¹) at the pump region, which gives another 49% increase in the THz power conversion efficiency. So compared with GaSe in the same crystal length, a 59% increase in the THz power conversion efficiency is theoretical gained by GaSe_{0.91}S_{0.09} due to the smaller reflective indices and absorption coefficient. This is well agreed with the practical efficiency enhancement of 45%.

In this letter, we have demonstrated a wide-band generation of the tunable high power monochromatic THz emission in a 5.5 mm-length 2 wt. % S-doped GaSe or solid solution GaSe_{0.91}S_{0.09} crystal by oe-e type DFG under the pump of Nd:YAG and OPO beams. When the PM angle is changed from 7.2° to 21.4° and the signal wavelength is in the range from 1066.3 to 1077.8 nm, the central wavelength of the terahertz emission is tuned from 528.0 to 84.0 μ m (0.57–3.57 THz). The achieved maximal output peak power is of 21.8 W at 1.62 THz (185.2 μ m), corresponding to the THz power conversion efficiency of 6.54×10^{-5} and photon efficiency of 1.14%. These efficiencies are well agreed with the theoretical calculations. And this THz power conversion

efficiency is 45% higher than that of pure GaSe crystal, which is mainly contributed to the improved optical properties. With these improved optical and mechanical properties, this terahertz source can be exploited for the out-of-door applications. Further improvement in the efficiency is possible by optimization of the crystal and pump beams parameters like large beam overlap and tight focusing.

The authors thank for the National Natural Science Funds in China (No. 61274138), Projects VIII.80.2.4 and MIPFI No. 46 SB RAS, and RFBR Nos.12-02-33174 and 13-02-0067.

- ¹J. Federici and L. Moeller, *J. Appl. Phys.* **107**, 111101 (2010).
- ²Y. C. Shen, L. Gan, M. Stringer, A. Burnett, K. Tych, H. Shen, J. E. Cunningham, E. P. J. Parrott, J. A. Zeitler, L. F. Gladden *et al.*, *Appl. Phys. Lett.* **95**, 231112 (2009).
- ³T. Yasui, Y. Kabetani, Y. Ohgi, S. Yokoyama, and T. Araki, *Appl. Opt.* **49**, 5262 (2010).
- ⁴W. Shi, Y. J. J. Ding, N. Fernelius, and K. Vodopyanov, *Opt. Lett.* **27**, 1454 (2002).
- ⁵Yu. M. Andreev, G. A. Verozubova, A. I. Gribenyukov, and V. V. Korotkova, *J. Korean Phys. Soc.* **33**, 356 (1998).
- ⁶Y. J. J. Ding, *IEEE J. Sel. Top. Quantum Electron.* **13**, 705 (2007).
- ⁷Y. J. Ding and W. Shi, *Solid State Electron.* **50**, 1128 (2006).
- ⁸K. Suizu, K. Miyamoto, T. Yamashita, and H. Ito, *Opt. Lett.* **32**, 2885 (2007).
- ⁹W. Shi and Y. J. J. Ding, *Appl. Phys. Lett.* **84**, 1635 (2004).
- ¹⁰Z. H. Kang, J. Guo, Z. S. Feng, J. Y. Gao, J. J. Xie, L. M. Zhang, V. Atuchin, Y. Andreev, G. Lanskii, and A. Shaiduko, *Appl. Phys. B: Lasers Opt.* **108**, 545 (2012).
- ¹¹Z.-S. Feng, Z.-H. Kang, F.-G. Wu, J.-Yu. Gao, Yu. Jiang, H.-Z. Zhang, Yu. M. Andreev, G. V. Lanskii, V. V. Atuchin, and T. A. Gavrilova, *Opt. Express* **16**, 9978 (2008).
- ¹²S.-A. Ku, W.-C. Chu, C.-W. Luo, Yu. Andreev, G. Lanskii, A. Shaiduko, T. Izaak, and V. Svetlichnyi, *Opt. Express* **20**, 5029 (2012).
- ¹³J. Guo, J.-J. Xie, L.-M. Zhang, D.-J. Li, G.-L. Yang, Yu. M. Andreev, K. A. Kokh, G. V. Lanskii, A. V. Shabalina, A. V. Shaiduko, and V. A. Svetlichnyi, *Cryst. Eng. Comm.* **15**, 6323–6328 (2013).
- ¹⁴Y.-K. Hsu, C.-W. Chen, J. Y. Huang, C.-L. Pan, J.-Y. Zhang, and C.-S. Chang, *Opt. Express* **14**, 5484–5491 (2006).
- ¹⁵Y. F. Zhang, R. Wang, Z. H. Kang, L. L. Qu, Y. Jiang, J. Y. Gao, Y. M. Andreev, G. V. Lanskii, K. A. Kokh, A. N. Morozov *et al.*, *Opt. Commun.* **284**, 1677 (2011).
- ¹⁶C. W. Luo, S. A. Ku, W. C. Chu, Yu. M. Andreev, V. V. Atuchin, N. F. Beizel, G. V. Lanskii, A. N. Morozov, and V. V. Zuev, in *IEEE Region 8 International Conference on Computational Technologies in Electrical and Electronics Engineering (SIBIRCON)* (2010), p. 576.
- ¹⁷M. M. Nazarov, A. P. Shkurinov, A. A. Angeluts, and D. A. Sapozhnikov, *Radiophys. Quantum Electron.* **52**, 536 (2009).
- ¹⁸J. X. Lu, B. B. Wang, J. G. Huang, Z. M. Huang, and X. M. Shen, *Proc. SPIE* **8195**, 819513 (2011).
- ¹⁹S. A. Ku, C. W. Luo, H. L. Lio, K. H. Wu, J. Y. Juang, A. I. Potekaev, O. P. Tolbanov, S. Y. Sarkisov, Y. M. Andreev, and G. V. Lanskii, *Russ. Phys. J.* **51**, 1083 (2008).
- ²⁰K. L. Vodopyanov and L. A. Kulevskii, *Opt. Commun.* **118**, 375 (1995).
- ²¹Y. R. Shen, *Nonlinear Infrared Generation* (Springer, New York, 1977), p. 28.